Journal of Radioanalytical and Nuclear Chemistry (2023) 332:2487–2497
https://doi.org/10.1007/s10967-023-08937-x

Uranium capture from aqueous solution using cement kiln dust; equilibrium and kinetic studies

Ahmed M. Masoud[1] · **M. M. El-Maadawy**[1] · **Mohamed H. Taha**[1] · **Amr Meawad**[2]

Received: 6 October 2022 / Accepted: 4 May 2023 / Published online: 24 May 2023

Abstract
Contamination of aquatic ecosystems with radioactive nuclides is significantly threaten the human body. So, finding effective and economical sorbents is significant for uranium elimination from an aqueous solution is important. In this study, Cement kiln dust (CKD) is a solid waste produced during the cement production process was utilized as sorbent for the uranium sorption from an aqueous solution. The maximum adsorption of 156.2 mg g^{-1} at pH 3.0 which reflects good sorption properties for the CKD. All in all, the displayed data declares that the CKD material possess an extraordinary tendency for U(VI) recovery from aquatic environments.

Keywords Cement kiln dust · Sorption · Uranium · Equilibrium · Kinetic

Introduction

Environmental pollution of radioactive metals that caused by anthropogenic behaviors released into the environment is one of the major challenges in modern human society [1, 2]. Radionuclides have gained wide public attention due to their chemical toxicity and radiotoxicity. Uranium, as the critical foundation resource of nuclear energy, can be simply found in the eco-system as a result of several nuclear activities, for example, uranium mining, milling and nuclear reactor waste [3, 4]. Worryingly, uranium is transferred to human body through the food chain [5]. Once consumed above the allowed uranium levels, it could result an enhanced risk of physical distortions and many diseases [6]. Hence, the recover and eliminate uranium from polluted water ecologically is important [7].

Well-established approaches for U(VI) recovery and capture from radioactive waste solutions have been performed for instance, include solvent extraction [8], chemical precipitation [9], reverse osmosis [10], micellar ultrafiltration [11], and ion exchange [12] are applied. Nevertheless, the performed approaches suffer from numerous drawbacks, for example these approaches limitations of these methods, such as incomplete removal, secondary pollution, and high energy consumption [13]. Meanwhile, adsorption as a simple, and cost effective technique has been widely applied for radionuclides capture from aqueous solutions [14–16].

Recently, attention has been focused on various adsorbents with metal-binding capacities and low costs, such as chitosan [17], zeolites [18], clay [19], or certain recycled materials like waste rubber [20], and cement kiln dust (CKD) [21].

CKD is yield as a side-product from the process of cement manufacturing. CKD, in large quantity, exit from the rotatory furnace, then separated by electrical filters, and finally stored [22]. Over the past years, efforts have been made to restructure the CKD to produce sustainable, high-quality, and environmentally friendly replacement sorbents for removing hazards from drinking as well as wastewater [23–26].

In this study, we aim to utilize CKD as the main adsorbent for the uptake of uranium from an aqueous solution. Optimization the main variables on U(VI) sorption process, and investigating the process kinetic and isotherm.

✉ Ahmed M. Masoud
chemmaso010@hotmail.com

✉ M. M. El-Maadawy
elma3dawi@yahoo.com

[1] Nuclear Materials Authority, El Maddi, P.O. Box 530, Cairo, Egypt

[2] Chemistry Department, Faculty of Science, Helwan University, Cairo 11795, Egypt

Experimental procedures

Materials

The reagents used were analytical grade and used without further purification. U(VI) solutions (1000 mg L^{-1}) was prepared from $UO_2(NO_3)_2 \cdot 6H_2O$ using double distilled water. Freshly collected CKD was obtained from Suez Cement Company in Cairo and used as a reactive adsorbent in batch experiments. Sophisticated instruments were applied for characterization the applied CKD sample to figure out its physical as well as chemical characteristics.

The chemical composition of the CKD sample was displayed using X-ray Fluorescence (XRF) spectroscopy (Axios, sequential WD-XRF spectrometer, PANalytical), while its phase composition was determined using X-ray diffraction (XRD, PANalytical Xpert Pro MRD Diffractometer, Amsterdam, Netherlands). Fourier transform infrared (ATR-FTIR) spectroscopy (Spectrum Two IR Spectrometer—PerkinElmer) was used to evaluate the chemical bonds and molecular vibrations at wavenumber of 4000 to 400 cm^{-1} by 64 scans and 4 cm^{-1} resolution. Zeta potential was determined using Zetsizer (Nicomp ZLS 380, USA) at 18°. The particle size distribution was explored using NICOMP 380 ZLS, Dynamic light scattering (DLS) instrument (PSS, Santa Barbara, CA, USA), using 632 nm line of a HeNe laser as the incident light with angel 90°. The Blaine surface area is measured by the air permeability apparatus.

Sorption methodology

The adsorption experiments have been studied by a batch technique in a thermostatic shaker bath model G.F.L 1083, Germany. The shaking rate was constant for all the experiments. The adsorbent material (CKD) (m, g) and a standard aqueous solution of uranium (V, L) were shaken at different temperatures for various mixing times. The pH of the aqueous solutions was maintained by Thiel buffer solution in the pH range (1–6). Filtration of the solid phase from liquid was followed by centrifuging at 4000 rpm for 5 min. ICP-AES was applied for measuring the residual concentrations of U(VI) (Ce, mg L^{-1}). All experiments were carried out twice, and mean values of 4% relative errors were used. U(VI) sorption capacity (qe, mg g^{-1}), sorption percent (%), and the distribution coefficient (kd) were evaluated using Eqs. 1–3 respectively:

$$q_e = \left(C_o - C_e\right) \times \frac{V}{m} \tag{1}$$

$$\text{U(VI) removal percent} = \frac{C_o - C_e}{C_o} \times 100 \tag{2}$$

Table 1 Chemical composition of CKD

Chemical composition	Weight (%)
SiO_2	12.14
Al_2O_3	3.57
Fe_2O_3	2.46
CaO	45.87
MgO	1.48
Na_2O	1.87
K_2O	4.76
SO_3	5.81
Cl^-	4.63
Free lime	18.10
L.O.I	14.9

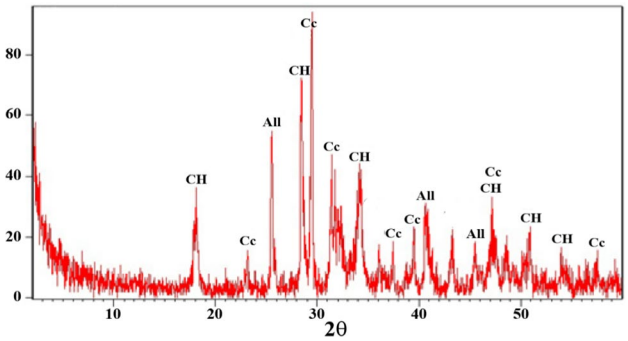

Fig. 1 XRD pattern of CKD (CH = portlandite, Cc = Calcite, All = Anhydrate)

$$K_d = \frac{\left(C_o - C_e\right)}{C_e} \times \frac{V}{m} \tag{3}$$

Results and discussions

Characterization of CKD

Calcium oxide was found to be the major oxide in the CKD while silica, alumina and iron oxide were the minor components, Table 1. The result confirmed the highly alkaline constituent of CKD with loss of ignition of 14.9% which attributed to the carbonation.

The mineralogical-based composition of CKD is carbonate from limestone and other inorganic oxides from clay as shown in Fig. 1.

Scanning electron microscopy with energy dispersive X-ray analysis (SEM-EDXA) (Device name) is a particularly useful tool for visual conformation of surface morphology and elemental analysis. SEM image of raw CKD, Fig. 2,

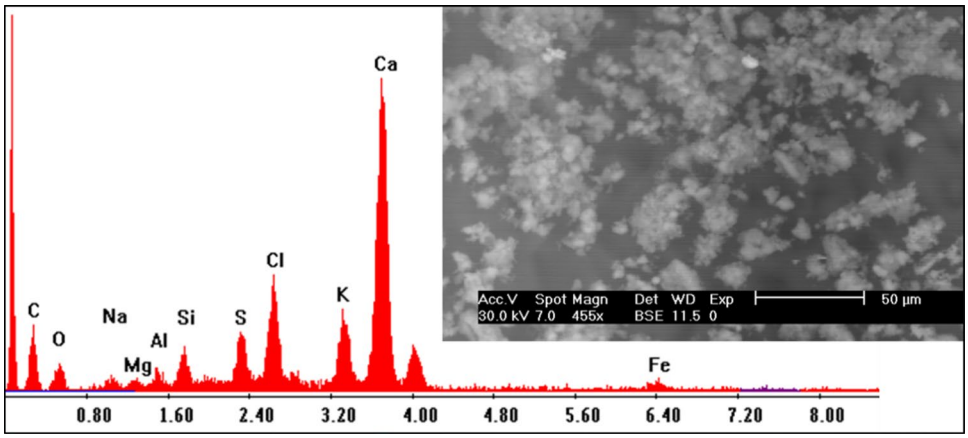

Fig. 2 SEM-EDXA of raw CKD

revealed irregular shape particles distributed heterogeneously. Also, porous structure of different sizes is observed. The EDXA spectrum confirmed that Ca, Si, Al, S, and K as majors while Fe, Na, Mg and Cl as minors elements.

The FTIR spectrum of CKD, Fig. 3, illustrates the stretching vibration frequency peak of the OH^- group exist at 3640 cm^{-1}. The stretching vibration frequency of H—O—H is appears at 3450 cm^{-1}, while the bending and stretching vibration frequency at 1435 and 877 cm^{-1} attributed to CO_3^{2-} group. The wave number of 1157 cm^{-1} belongs to the Ca-O group which could be due to the free CaO.

The particle size distribution, zeta potential and surface area are keys in determining the efficacy of CKD in the removal of uranium. Figure 4 shows the distribution of CKD particle size with a mean diameter of 15 µm while zeta potential is found to be − 0.32 mV. The measured Blaine surface area is 4550 cm^2/g.

Sorption of uranium (VI) using CKD

Uranium (VI) sorption from aqueous solution using CKD material has been investigated. The sorption performance of CKD was explored by investigating the sorption kinetics, isotherm, and thermodynamics. Uranium desorption from the loaded CKD as well as the utilization of the CKD for radioactive liquid effluent treatment was performed.

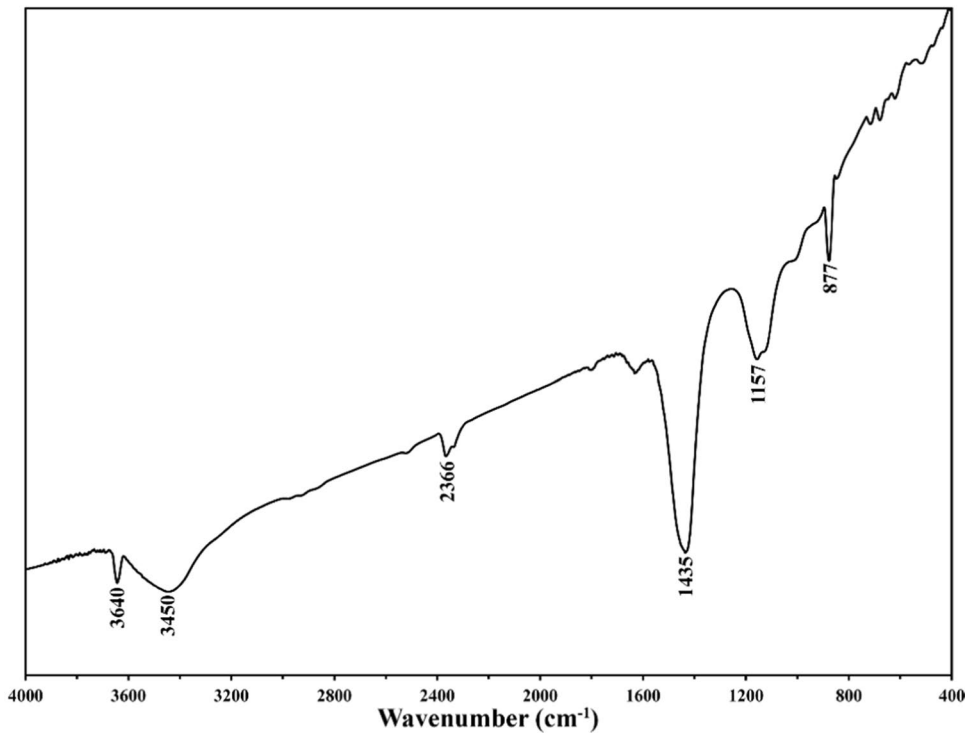

Fig. 3 FTIR spectrum of CKD

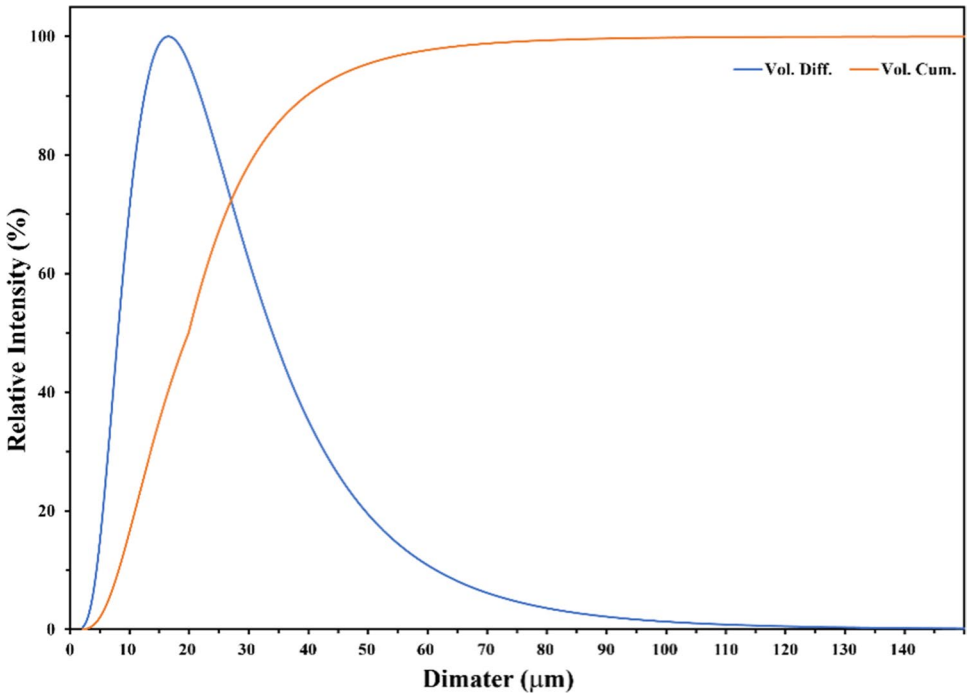

Fig. 4 Particle size distribution of CKD

Contact time and sorption kinetics

The kinetics as well as U(VI) sorption mechanism could be assessed by investigating the impact of contact time of the sorption process. In accordance, numerous tests were conducting at fixed sorbent dose of 0.3 g/ L, solution pH of 3.2, room temperature, and U(VI) initial concentration of 50 mg L^{-1}, and reaction time interval of 2–120 min. It can be noticed from Fig. 5 that U(VI) sorption process characterized by fast kinetic performance whereas the sorption capacity increased sharply (from 52 to 133 mg g^{-1}) by increment of reaction time up to 15 min (equilibrium state). This performance could be attributed to the availability, in large number, of the vacant surface-active sites for U(VI) adsorption [27]. Beyond a reaction time of 15 min, a slightly change in the sorption capacity was recognized. The gradual

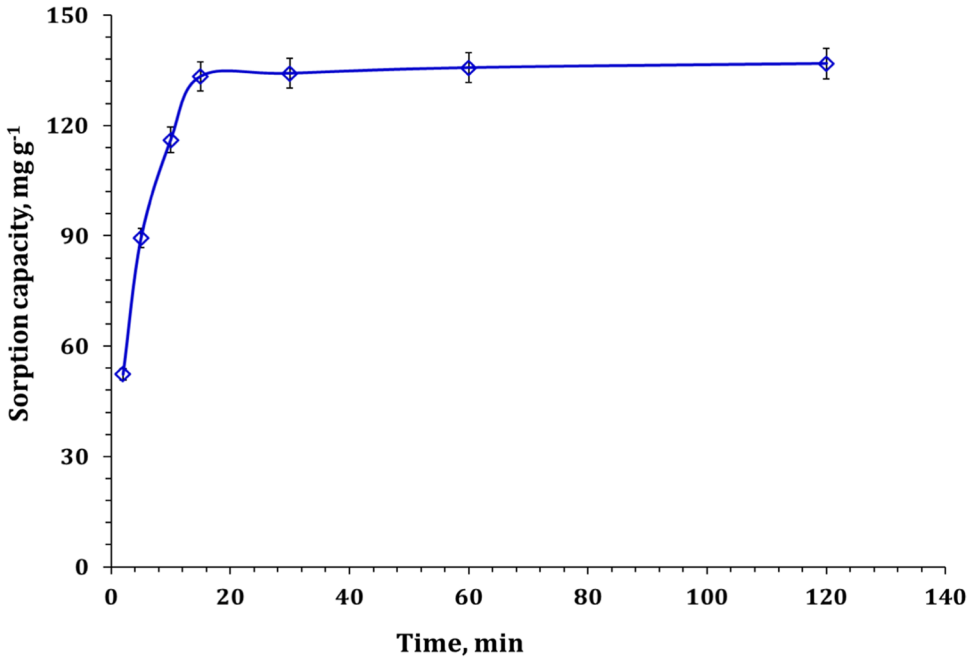

Fig. 5 Effect of time on the sorption percent, % (solution pH of 3.2, room temperature, U(VI) initial concentration of 50 mg/ L, sorbent dose of 0.3 g L^{-1})

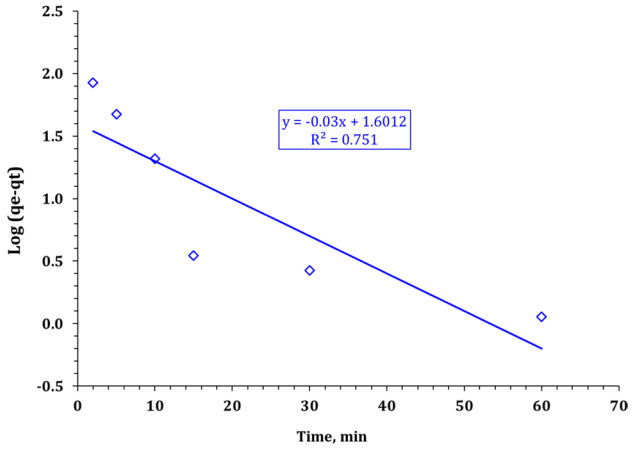

Fig. 6 Pseudo-first-order plot for uranium sorption using CKD

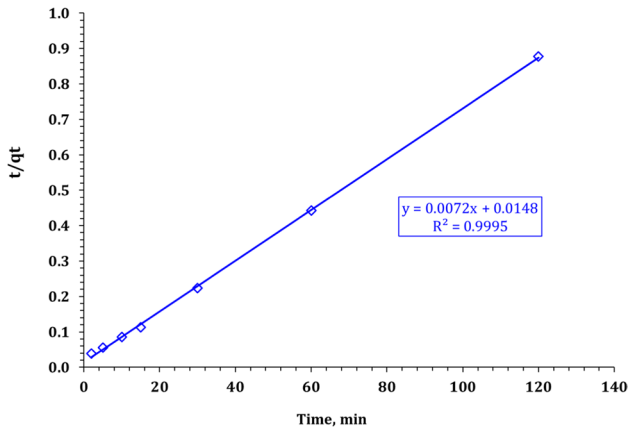

Fig. 7 Pseudo second-order plot for U(VI) sorption using CKD

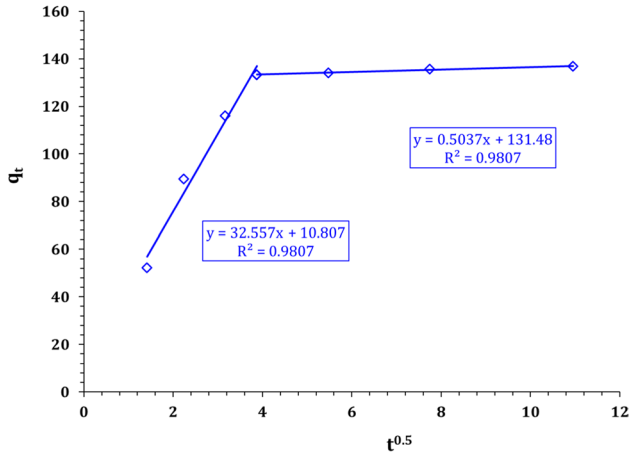

Fig. 8 Morris-Weber plot for U(VI) sorption using CKD

Table 2 The calculated parameters of the applied kinetic models

Lagergreen pseudo first-order	k_1 (min^{-1})	0.238
	qe_{cal} (mg/g)	156.5
	qe_{exp} (mg/g)	136.8
	R^2	0.96
Pseudo second-order	K_2 (min^{-1})	0.004
	qe_{cal} (mg/g)	138.9
	qe_{exp} (mg/g)	136.8
	H (mol g^{-1} h^{-1})	67.57
	$t_{1/2}$ (h)	2.1
	R^2	0.99
Weber and morris model	Stage I	
	k_i(mg/g $min^{1/2}$)	32.56
	C	32.6
	R^2	0.98
	Stage II	
	k_i (mg/g $min^{1/2}$)	0.50
	C	131.5
	R^2	0.98

decrease in reaction rate could be owned to the decrease of active function groups on the CKD surface over time [28].

The sorption kinetic profile was explored in detail by fitting the attained results using three conventional kinetic models, namely; Lagergreen (pseudo- first-order), pseudo-second-order, and Weber-Morris (W-M). Table S1 declares the linear forms of the applied models [29, 30]. Lagergreen kinetic model plot (log (qe-qt) against reaction time), pseudo-second-order mode plot (t/ qt verses reaction time), and *Morris-Weber* (qt as a function of $t^{0.5}$) were exhibited in Figs. 6, 7 and 8 respectively, and the kinetic parameters were evaluated and declared in Table 2.

The displayed data in Table 2 declare that pseudo-second-order kinetic models showed higher value for the correlation coefficient R^2, reflecting more fitting with the experimental results than pseudo-first order. Furthermore, the calculated sorption capacity from the pseudo-second-order kinetic model is nearer to the experimental value. These results reflect that U(VI) sorption results using CKD are highly fitted with the pseudo-second-order. This indicates that the uranium uptake with CKD is a chemisorption process, and the reaction involves an electron sharing between the uranium species and the sorbent active sites [29, 30]. The half initial sorption rate (h: 67.5 mol g^{-1} h^{-1}) and the equilibrium time ($t_{1/2}$: 2.1 h) confirming the fast kinetic rate of reaction for the uranium sorption process. CKD shows the same kinetic attitude during the removal of Cd(II) from aqueous solution [31].

Weber-Morris kinetic model showed that the adsorption process is controlled by two steps, where the relation between q_t and $t^{0.5}$ showed two linear stages Fig. 8, which reflect that more than one mechanisms participating in the

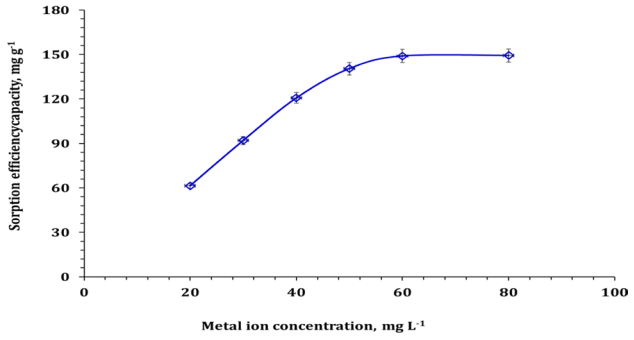

Fig. 9 U(VI) sorption percent as a function of initial concentration (reaction time 30 min; temperature 25 ± 1 °C; 0.3 g sorbent/ L)

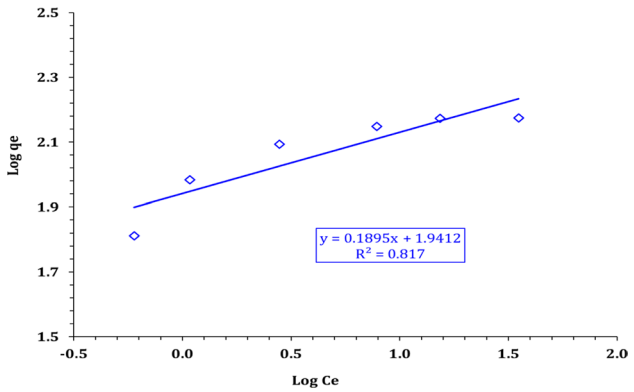

Fig. 10 Freundlich isotherm plot for U(VI) sorption using CKD

adsorption process [29, 30]. The first linear stage shows high rate of reaction which could be attributed to the availability of active sites on the adsorbent surface, however the second linear stage characterized by slow rate of reaction which could be attributed to the saturation of adsorbent surface active sites. The results declare that the intra-particle diffusion mechanism (pore or surface diffusion) take part with the effect of U(VI) concentration gradient [32, 33].

Initial concentration and isotherm investigation

Figure 9 exhibits the variation of uranium capacity from aqueous medium using CKD material verses U(VI) initial concentration range (20–80 mg L^{-1}). The anticipated results show the enhancement of U(VI) sorption capacity with the increment of uranium initial concentration up to 60 mg/ L followed by by steady stat due to sorbent saturation. The saturation plateau indicating uranium binding to the CKD material could be occurred as a monolayer [32, 33].

Langmuir and Freundlich isotherm models had been utilized to explore in detail the isotherm of U(VI) sorption using CKD material. Table S1 displayed the linear

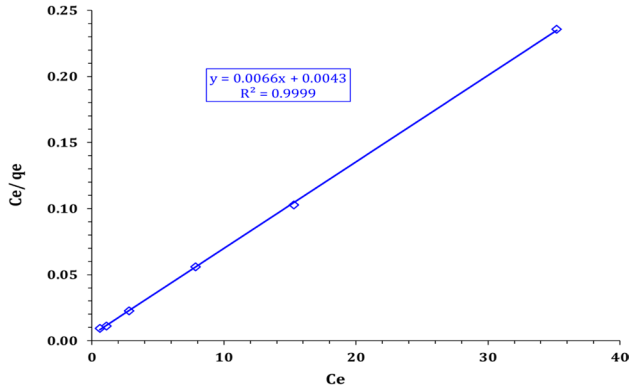

Fig. 11 Langmuir isotherm graph for U(VI) sorption using CKD

Table 3 Freundlich and Langmuir isotherm parameters for U(VI) sorption using CKD

Freundlich isotherm odel	n		3.88
	k_f (mg/ g)		70.68
	R^2		0.74
Langmiur isotherm model	Q_m (mg/g)		156.25
	b (L/mg)		0.674
	R^2		0.99
	RL	Co, mg^{-1}	
		20	0.069
		30	0.047
		40	0.036
		50	0.029
		60	0.024
		80	0.018

form of the kinetic equations [34, 35]. Figure 10 (Ce/ qe against Ce) was used to obtained Langmuir isotherm parameters, while the parameters of Freundlich isotherm model (Fig. 11) were determined from the variation of log q_e as a function of log Ce. Table 3 exhibit the attained isotherm parameters values Table 3.

The provided data declare that U(VI) removal using CKD is described well with Langmuir isotherm model ($R^2 = 0.99$) which indicates that the uranium sorption is a monolayer cover. The same isotherm performance was reported for Cu, and Zn sorption from aqueous solution using CKD material [36].

Uranium(VI) sorption capacity using CKD was displayed in Table 4 in comparison with other materials sorption capacities. Table 4 declares that CKD materials possess uranium sorption capacity within the obtained from literature, which reflects that CKD is a promising sorbent for considered as potential materials for radioactive waste treatment.

Table 4 Experimental results of adsorption capacity of CKD compared with those of some other adsorbents, for uranium sorption from aqueous solution, based on literature

	qe, mg g^{-1}	Ref
Polyacrylamide-based chelating polymer I	65.3	[37]
Poly (acrylamide-acrylic acid)-titanium silicate (P-(AM-AA)-TS) composite	64.1	[38]
PA6/n-HAp	116.62	[39]
Purolite A400 anion Exchange resin	117.6	[40]
TBP immobilised PVC cement	17.4	[41]
Amberjet 1200 H cation exchange resin	133	[42]
CKD	156.2	Present work

Temperature and thermodynamic investigation

The impact of reaction temperature is an important parameter to display the sorption nature as well as the thermodynamic parameters of the sorption process. In this regard, a set of experiments were conducted reaction temperature interval of 25–50 ± 1 °C, and reaction time of 30 min, pH 3.1, 50 mg L^{-1} initial concentration, and 0.3 g L^{-1} sorbent dose.

The collected data from Fig. 12 declare the endothermic nature of uranium sorption process whereas, U(VI) sorption capacity is gradual increased by increasing the reaction temperature, which reflects the endothermic nature of the U(VI) sorption process using CKD. This performance could be attributed to increase the U(VI) species driving forces, and the probability of U(VI) interaction with the CKD surface active sites, as the reaction temperature raises [43].

The thermodynamic equations displayed in Table S1 [44] were applied to assess the thermodynamic variables i.e. standard free energy change (ΔG^o, kJ/mol), standard enthalpy change (ΔH^o, kJ/mol), and standard entropy change (ΔS^o, J/(mol.K)). Illustrate of log Kc *VIS* 1/T is displayed in Figure S1, while the values of the thermodynamic parameters were exhibited in Table 5.

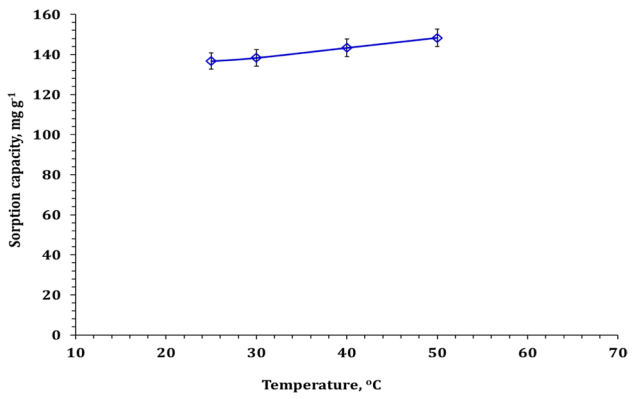

Fig. 12 Effect of temperature on the U(VI) sorption efficiency, % (0.3 g sorbent/ L; reaction time 30 min; 50 mg L^{-1} initial concentration)

The displayed data in Table 5 obvious the positive ΔH^o value which indicating an endothermic sorption process. Furthermore, the feasible and spontaneous nature for the sorption process could be recognized from the negative values of the ΔG^o over the investigated reaction temperature range. In addition, the increase of randomness at the sorbent/ adsorbents interfaces could be indicated from the positive values of entropy change (ΔS^o) [32, 43].

Uranium sorption mechanism

CKD possess high efficiency for heavy metal removal from contaminated aqueous solutions owned to its high surface area, alkalinity, oxide, and carbonate content [45]. The removal of heavy metals using CKD could involve several mechanisms. (1) Adsorption mechanism, which is predominantly at low metal concentration and occur at certain pH value and attributed to the fine texture and oxide components of the CKD material [46]. This mechanism involves the surface complexation between the metal ions and the oxides on the rough surface of the CKD fine particles [47, 48]. (2) Precipitation mechanism, which is predominantly at high metal ion concentration [49]. This mechanism is owned to the high pH and lime content of CKD which dissolve in the aqueous solution, and in turn increases the solution pH above the metal ions solubility point (formation of metal hydroxide precipitate) [50, 51]. (3) Sorption/ precipitation interaction, where both mechanisms could be involved during the metal ions capture using CKD whereas these metal ions could be sorbet on the metal oxides existing on the CKD surface and could be precipitate due to the high alkali oxides content in the CKD [52, 53].

In the present study, the kinetic analysis (Weber-Morris model) reflects that the U(VI) uptake process is controlled with multiple mechanisms (Fig. 8). According to the XRF analysis of the applied CKD sample (Table 1) it is clear that the CKD possess high oxides components which suggests the formation of surface complexation between uranium species and the surface-active sites oxides such as Si–OH, Al–OH, Fe–OH. Kinetic analysis for the anticipated data declares that U(VI) removal process is fitted to Pseudo-second order kinetic model which indicates that the uptake process is chemisorption and involves the electron

Table 5 Thermodynamic parameters for U(VI) sorption using CKD

ΔG (kJ/ mol)				ΔH (kJ/ mol)	ΔS (kJ/ mol)
25 °C	30 °C	40 °C	50 °C		
− 23.86	− 24.43	− 25.84	− 27.40	18.60	142.48

sharing between the CKD surface active sites and uranium molecules. This finding confirms the complexation interaction between uranium species and the CKD surface oxides (inner-sphere surface complexation mechanism). Uranium species is mainly present as cationic species (UO_2^{2+}) at the studied solution pH (~3.0) [41], and Fig. 3 displays that CKD exhibit negative surface charge (−0.32 mV) which obvious that the electrostatic attraction between the positive uranium species and negative CKD surface could take place during the sorption process (electrostatic interaction mechanism). Furthermore, the high content of free lime in the CKD sample (Table 1) reflects that increase of solution pH which indicates that the precipitation mechanism could also control the uranium capture process due to the conversion of uranium species to the insoluble form. The multiple interaction mechanism of CKD material is also reported for heavy metal removal from wastewater [47, 54].

After performing the capture of uranium species by CKD, some differences could be observed in the FTIR of spent adsorbent compared to the raw CKD, as presented in Fig. 13. Three absorption bands could be stretching more intensely at 1435, 1157 and 877 cm^{-1} referring to the complex formation between U(VI) molecules and the donating function groups in CKD. Furthermore, disappearing in the identifying absorption band for O–H group could be noted the provided FTIR spectrum. Its intensity and broadness could be strongly affected which can be attributed to the complexation between OH^- group and uranium ions which are attached on the surface of the adsorbent. The observed variations in the FTIR spectrum of spent adsorbent, compared to its corresponding raw one, can confirm the successful removal of uranium species by the introduced structure.

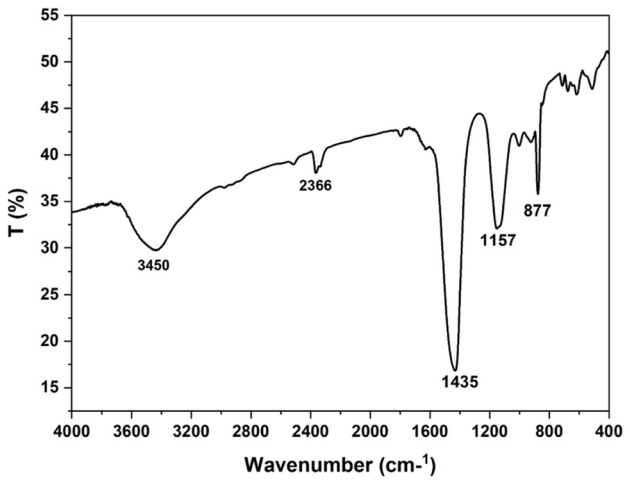

Fig. 13 FTIR spectrum of CKD after uranium adsorption

The removal of uranium species from the liquid media was further verified through SEM analysis, as shown in Fig. 14. The noticeable difference in the shape of the applied absorbent, compared to the raw CKD, can be observed in the selected SEM image. In particular, a quite compact accumulated layers with no observed pores were observed on particles surface for CKD-U(VI), compared with virgin-CKD absorbent. This observation may be due to formation of monolayer adsorbed U(VI) on the surface of CKD, which agreed with Langmuir isotherm model results. Additionally, the EDXA analysis confirms U(VI) adherence onto CKD surface where a new peak of uranium appeared in the EDX spectrum.

Uranium desorption investigation

Uranium recovery from the loaded CKD was performed using several desorption solutions i.e., HCl, HNO_3, and H_2SO_4 at 25 °C (Table S2). Initially, the loaded CKD was treated with 50 mL of 1.0 M of every eluting solution for 2 h, sorbent dosage of 0.3 g/ L at room temperature. The attained results declare that better desorption (~92%) when nitric acid is applied. Therefore, HNO_3 was chosen for recovering U(VI) ions as the greatest desorbing agent.

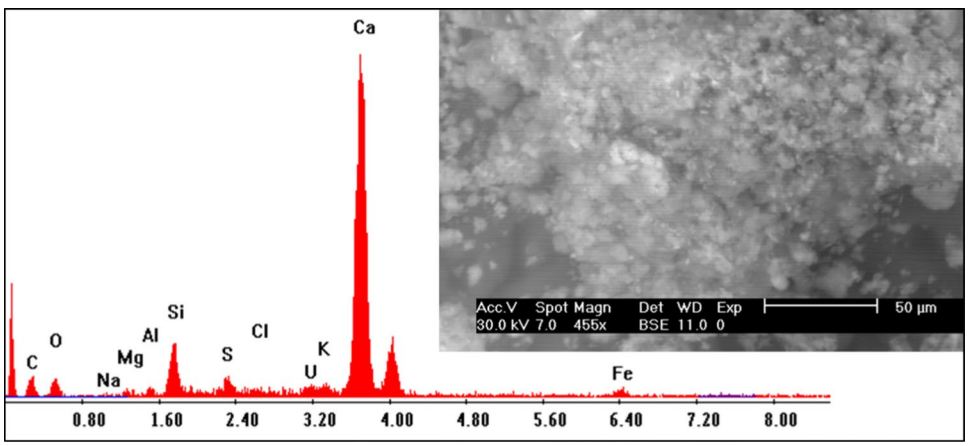

Fig. 14 SEM-EDXA of CKD after uranium adsorption

Uranium removal from the liquid raffinate solution (Case study)

Removal of uranium from waste solution is an imperative procedure from the ecological point of view. Consequently, CKD sorbent undergoes an application experiment to eliminate uranium ions from a liquid waste solution supplied from the Nuclear Materials Authority, Egypt. ICP-AES was applied to explore the waste effluent chemical composition, and found to be: Fe(III) and Ca(II) concentrations of 1.84 and 0.63 g L^{-1} respectively, 1.0 M nitric acid concentration, and 60 mg/ L uranium concentration. The experimental parameters were: pH of 3.1, CKD amount of addition 0.3 g/ L, room temperature, and reaction time of 30 min. The obtained data indications that about 93% of the uranium content in the raffinate sample was effectively removed, which suggests that CKD material is a promising sorbent for radioactive waste treatment.

Conclusions

The present study showed that CKD adsorbent has considerable efficiency for uranium ions elimination from an aqueous solution. The equilibrium adsorption is practically achieved in 15 min. Moreover, it was a function of temperature and U(VI) concentration. The kinetic study for U(VI) adsorption onto CKD revealed that the adsorption kinetics adapts with pseudo-second-order model. The experimental adsorption results fitted well with Langmuir isotherm model with maximum adsorption capacity of 156.25 mg g^{-1}. The thermodynamic parameters (ΔH, ΔS°, and ΔG°) revealed the spontaneous and endothermic nature of the adsorption process. Conclusively, the present study infers that the CKD could be utilized as low-cost adsorbents for the uranium from wastewater.

Supplementary Information The online version contains supplementary material available at https://doi.org/10.1007/s10967-023-08937-x.

Funding Open access funding provided by The Science, Technology & Innovation Funding Authority (STDF) in cooperation with The Egyptian Knowledge Bank (EKB).

Declarations

Conflict of interest The authors of this manuscript have no competing or conflict of interest with any person or any organization.

References

1. Youssef WM, Hussein AEM, Taha MH, El-Maadawy MM (2022) Uranium(VI) sorption from liquid waste solution using functionalized polyurethane polymer: kinetic and isotherm characterizations. Russ J Inorg Chem 677(67):1058–1068. https://doi.org/10.1134/S0036023622070245
2. Briffa J, Sinagra E, Blundell R (2020) Heavy metal pollution in the environment and their toxicological effects on humans. Heliyon 6:e04691. https://doi.org/10.1016/J.HELIYON.2020.E04691
3. Howari F, Salman A, Goodell P (2022) Uranium resources in the Middle East and North Africa. Uranium Geol Middle East North Africa. https://doi.org/10.1016/B978-0-323-90992-1.00005-1
4. Akash S, Sivaprakash B, Raja VCV et al (2022) Remediation techniques for uranium removal from polluted environment—review on methods, mechanism and toxicology. Environ Pollut 302:119068. https://doi.org/10.1016/J.ENVPOL.2022.119068
5. Balaram V, Rani A, Rathore DPS (2022) Uranium in groundwater in parts of India and world: a comprehensive review of sources, impact to the environment and human health, analytical techniques, and mitigation technologies. Geosyst Geoenviron 1:100043. https://doi.org/10.1016/J.GEOGEO.2022.100043
6. Abd El-Magied MO, Hassan AM, El-Aassy IK et al (2021) Development of functionalized activated carbon for uranium removal from groundwater. Int J Environ Res 15:543–558. https://doi.org/10.1007/S41742-021-00333-1/TABLES/9
7. Kumar M, Seth A, Singh AK et al (2021) Remediation strategies for heavy metals contaminated ecosystem—a review. Environ Sustain Indic 12:100155. https://doi.org/10.1016/J.INDIC.2021.100155
8. Ali MM, Taha MH, Killa HM et al (2014) Synergistic extraction of uranium from acidic sulfate leach liquor using D2EHPA mixed with TOPO. J Radioanal Nucl Chem 300:963–967. https://doi.org/10.1007/S10967-014-3094-1/TABLES/2
9. Biswas S, Rupawate VH, Hareendran KN et al (2015) Novel precipitation technique for uranium recovery from carbonate leach solutions. J Radioanal Nucl Chem 304:1345–1352
10. Shen J, Schäfer A (2014) Removal of fluoride and uranium by nanofiltration and reverse osmosis—a review. Chemosphere 117:679–691. https://doi.org/10.1016/J.CHEMOSPHERE.2014.09.090
11. Shojaei H, Keshtkar A, Moosavian M, Torkabad MG (2021) Modeling uranium (II) removal from aqueous solution by micellar enhanced ultrafiltration using response surface methodology. Groundw Sustain Dev 15:100660. https://doi.org/10.1016/J.GSD.2021.100660
12. Taha MH (2020) Solid-liquid extraction of uranium from industrial phosphoric acid using macroporous cation exchange resins: MTC1600H, MTS9500, and MTS9570. Sep Sci Technol. https://doi.org/10.1080/01496395.2020.1787446
13. Younes AA, Masoud AM, Taha MH (2021) Amino-functionalised cross-linked polyacrylamide for the adsorption of U(VI) ions from contaminated aqueous solutions. Int J Environ Anal Chem. https://doi.org/10.1080/03067319.2021.2003348
14. Faiz Norrrahim MN, Mohd Kasim NA, Knight VF et al (2021) Nanocellulose: a bioadsorbent for chemical contaminant remediation. RSC Adv 11:7347–7368. https://doi.org/10.1039/D0RA08005E

15. Lekshmi R, Rejinie Mon TS, Sathya R et al (2022) Adsorption of heavy metals from the aqueous solution using activated biomass from Ulva flexuosa. Chemosphere 306:135479. https://doi.org/10.1016/J.CHEMOSPHERE.2022.135479
16. Masoud AM, Saeed M, Taha MH, El-Maadawy MM (2020) Uranium adsorption from Bahariya Oasis leach liquor via TOPO impregnated bentonite material; isothermal, kinetic and thermodynamic studies. Egypt J Chem 63:721–741. https://doi.org/10.21608/EJCHEM.2019.13638.1843
17. Liu W, Wang Q, Wang H et al (2022) Adsorption of uranium by chitosan/Chlorella pyrenoidosa composite adsorbent bearing phosphate ligand. Chemosphere 287:132193. https://doi.org/10.1016/J.CHEMOSPHERE.2021.132193
18. Ai Y, Yin N, Ouyang Y et al (2022) Waste non-burn-free brick derived sulfhydryl functioned magnetic zeolites and their efficient removal of uranium(VI) ions. Appl Surf Sci 571:151241. https://doi.org/10.1016/J.APSUSC.2021.151241
19. Cheng J, Gu R, He P et al (2022) Study on the uranium (U(VI)) adsorption stability of high-dose γ-ray-irradiated clay. Appl Radiat Isot 181:110102. https://doi.org/10.1016/J.APRADISO.2022.110102
20. Tan J, Wang Y, Liu N, Liu M (2018) Adsorption of uranium (VI) from aqueous solution by tetraphenylimidodiphosphinate. J Radioanal Nucl Chem 315:119–127
21. Hasaballah AF, Hegazy TA, Ibrahim MS, El-Emam DA (2021) Cement kiln dust as an alternative technique for wastewater treatment. Ain Shams Eng J 12:4201–4209. https://doi.org/10.1016/J.ASEJ.2021.04.026
22. Abbas RAH, Shehata N, Elrahman EA et al (2021) Environmental safe disposal of cement kiln dust for the production of geopolymers. Egypt J Chem 64:7529–7537. https://doi.org/10.21608/EJCHEM.2021.89060.4276
23. Naushad M, Vasudevan S, Sharma G et al (2015) Adsorption kinetics, isotherms, and thermodynamic studies for Hg^{2+} adsorption from aqueous medium using alizarin red-S-loaded amberlite IRA-400 resin. Desalin Water Treat 57:18551–18559. https://doi.org/10.1080/19443994.2015.1090914
24. Naushad M, Mittal A, Rathore M, Gupta V (2014) Ion-exchange kinetic studies for Cd(II), Co(II), Cu(II), and Pb(II) metal ions over a composite cation exchanger. Desalin Water Treat 54:2883–2890. https://doi.org/10.1080/19443994.2014.904823
25. Sulaymon AH, Faisal AAH, Khaliefa QM (2015) Cement kiln dust (CKD)-filter sand permeable reactive barrier for the removal of Cu(II) and Zn(II) from simulated acidic groundwater. J Hazard Mater 297:160–172. https://doi.org/10.1016/J.JHAZMAT.2015.04.061
26. Sulaymon AH, Faisal AAH, Khaliefa QM (2017) Dominant mechanisms for metal removal from acidic aqueous solutions by cement kiln dust. Mine Water Environ 36:209–216. https://doi.org/10.1007/S10230-016-0416-2/TABLES/2
27. Ghoochian M, Panahi HA, Sobhanardakani S et al (2019) Synthesis and application of Fe_3O_4/SiO_2/thermosensitive/PAMAM-CS nanoparticles as a novel adsorbent for removal of tamoxifen from water samples. Microchem J 145:1231–1240. https://doi.org/10.1016/J.MICROC.2018.12.004
28. Jain R, Peräniemi S, Jordan N et al (2018) Removal and recovery of uranium(VI) by waste digested activated sludge in fed-batch stirred tank reactor. Water Res 142:167–175. https://doi.org/10.1016/J.WATRES.2018.05.042
29. Largitte L, Pasquier R (2016) A review of the kinetics adsorption models and their application to the adsorption of lead by an activated carbon. Chem Eng Res Des 109:495–504. https://doi.org/10.1016/J.CHERD.2016.02.006
30. Kim YS, Kim JH (2019) Isotherm, kinetic and thermodynamic studies on the adsorption of paclitaxel onto Sylopute. J Chem Thermodyn 130:104–113. https://doi.org/10.1016/J.JCT.2018.10.005
31. El-Refaey AA (2016) Comparative performance of cement kiln dust and activated carbon in removal of cadmium from aqueous solutions. Water Sci Technol 73:1691–1699. https://doi.org/10.2166/WST.2015.651
32. Mishra V, Sureshkumar MK, Gupta N, Kaushik CP (2017) Study on Sorption characteristics of uranium onto biochar derived from eucalyptus wood. Water Air Soil Pollut 228:1–14. https://doi.org/10.1007/S11270-017-3480-8/FIGURES/9
33. Li M, Liu H, Chen T et al (2019) Synthesis of magnetic biochar composites for enhanced uranium(VI) adsorption. Sci Total Environ 651:1020–1028. https://doi.org/10.1016/J.SCITOTENV.2018.09.259
34. Kang HJ, Kim JH (2019) Adsorption kinetics, mechanism, isotherm, and thermodynamic analysis of paclitaxel from extracts of taxus chinensis cell cultures onto sylopute. Biotechnol Bioprocess Eng 243(24):513–521. https://doi.org/10.1007/S12257-019-0001-1
35. Foo KY, Hameed BH (2010) Insights into the modeling of adsorption isotherm systems. Chem Eng J 156:2–10. https://doi.org/10.1016/J.CEJ.2009.09.013
36. Sulaymon AH, Faisal AAH, Khaliefa QM (2014) Simultaneous adsorption–precipitation characterization as mechanisms for metals removal from aqueous solutions by cement kiln dust (CKD). Desalin Water Treat 57:819–826. https://doi.org/10.1080/19443994.2014.976769
37. Younes AA, Masoud AM, Taha MH (2018) Uranium sorption from aqueous solutions using polyacrylamide-based chelating sorbents. Sep Sci Technol 53:2573–2586. https://doi.org/10.1080/01496395.2018.1467450
38. Haggag ESA, Abdelsamad AA, Masoud AM (2019) Potentiality of uranium extraction from acidic leach liquor by polyacrylamide-acrylic acid titanium silicate composite adsorbent. Int J Environ Anal Chem 100:204–224. https://doi.org/10.1080/03067319.2019.1636037
39. Hassanein TF, Masoud AM, Mohamed WS et al (2021) Synthesis of polyamide 6/nano-hydroxyapatite hybrid (PA6/n-HAp) for the sorption of rare earth elements and uranium. J Environ Chem Eng 9:104731. https://doi.org/10.1016/J.JECE.2020.104731
40. Masoud AM (2020) Sorption behavior of uranium from Sulfate media using purolite A400 as a strong base anion exchange resin. Int J Environ Anal Chem. https://doi.org/10.1080/03067319.2020.1763974
41. Hussein AEM, Taha MH (2013) Uranium removal from nitric acid raffinate solution by solvent immobilized PVC cement. J Radioanal Nucl Chem 295:709–715. https://doi.org/10.1007/S10967-012-2158-3/TABLES/2
42. Khawassek YM, Masoud AM, Taha MH, Hussein AEM (2018) Kinetics and thermodynamics of uranium ion adsorption from waste solution using Amberjet 1200 H as cation exchanger. J Radioanal Nucl Chem 315:493–502. https://doi.org/10.1007/S10967-017-5692-1/FIGURES/13
43. Elzoghby AA, Bakry A, Masoud AM et al (2021) Synthesis of polyamide-based nanocomposites using green-synthesized chromium and copper oxides nanoparticles for the sorption of uranium from aqueous solution. J Environ Chem Eng 9:106755. https://doi.org/10.1016/J.JECE.2021.106755
44. Saha P, Chowdhury S (2011) Insight into adsorption thermodynamics. Thermodynamics. https://doi.org/10.5772/13474
45. Pesavento M, Profumo A, Alberti G, Conti F (2003) Adsorption of lead(II) and copper(II) on activated carbon by complexation with surface functional groups. Anal Chim Acta 480:171–180. https://doi.org/10.1016/S0003-2670(02)01597-0

46. Mahmoued EK (2010) Cement kiln dust and coal filters treatment of textile industrial effluents. Desalination 255:175–178. https://doi.org/10.1016/J.DESAL.2009.12.025
47. Shaheen SM, Eissa FI, Ghanem KM et al (2015) Metal ion removal from wastewaters by sorption on activated carbon, cement kiln dust, and sawdust. Water Environ Res 87:506–515. https://doi.org/10.2175/106143015X14212658614630
48. Amin AEEAZ, Selmy SAH (2017) Effect of pH on removal of Cu, Cd, Zn, and Ni by cement kiln dust in aqueous solution. Commun Soil Sci Plant Anal 48:1301–1308. https://doi.org/10.1080/00103624.2017.1341914
49. Aziz HA, Adlan MN, Ariffin KS (2008) Heavy metals (Cd, Pb, Zn, Ni, Cu and Cr(III)) removal from water in Malaysia: post treatment by high quality limestone. Bioresour Technol 99:1578–1583. https://doi.org/10.1016/J.BIORTECH.2007.04.007
50. Liu F, Zhou J, Jin T et al (2016) Effect of calcium oxide on the efficiency of ferrous ion oxidation and total iron precipitation during ferrous ion oxidation in simulated acid mine drainage treatment with inoculation of Acidithiobacillus ferrooxidans. Water Sci Technol 73:1442–1453. https://doi.org/10.2166/WST.2015.600
51. Mackie AL, Walsh ME (2012) Bench-scale study of active mine water treatment using cement kiln dust (CKD) as a neutralization agent. Water Res 46:327–334. https://doi.org/10.1016/J.WATRES.2011.10.030
52. Salem A, Velayi E (2012) Application of hydroxyapatite and cement kiln dust mixture in adsorption of lead ions from aqueous solution. J Ind Eng Chem 18:1216–1222. https://doi.org/10.1016/J.JIEC.2011.11.113
53. Klimantavièiûtë MG, Virbalytë D, Pakðtas V et al (2005) Interaction of heavy metal ions with cement kiln dust. EKOLOGIJA 1:31–36
54. Abd Ali ZT, Naji LA, Almuktar SAAAN et al (2020) Predominant mechanisms for the removal of nickel metal ion from aqueous solution using cement kiln dust. J Water Process Eng 33:101033. https://doi.org/10.1016/J.JWPE.2019.101033